Interrogating the mechanisms controlling sulfur isotope fractionation during sulfate reduction

DAVID T. JOHNSTON*, WILLIAM D. LEAVITT, MARIAN SCHMIDT, SCOTT D. WANKEL, ALEX S. BRADLEY AND PETER R. GIRGUIS

Harvard University, Dept. of Earth and Planetary Sciences, Cambridge, MA, USA, johnston@eps.harvard.edu (*presenting author)

The sedimentary sulfur isotope record represents a unique opportunity to learn about Earth's environmental history. This great interpretability is related to the fact that the sulfur cycle captures the interplay of numerous redox sensitive biological processes and preserves an extraordinary geological signal, both of which are accessible with a multiple isotope system. The precision with which we can tell these stories, however, rests with the quality of our calibrations. To date, isotopic calibrations have targeted microbial sulfate reduction; an anaerobic metabolism that is both the dominant contributor to the preserved sulfur isotope variability and provides the tight, quantitative links between the sulfur, oxygen and carbon cycles. Decades of classic batch experiments with whole cells of sulfate reducers underpin our understanding of the fractionation capacity of this metabolism, coarsely linking cellular and volumetric rates of reduction to the inverse of the magnitude of $^{34}S/^{32}S$ fractionation (*1*). Although informative, it is possible to both place tighter quantitative constraints on this relationship, as well as to develop a more fundamental understanding of the physiological mechanisms driving the observed fractionation patterns. With this level of calibration, and through the inclusion of minor isotope fractionation patterns, a more refined picture of Earth surface evolution is possible.

In what follows we present data from a suite of continuous culture experiments with two pure *Desulfovibrio* strains of sulfate reducer: *D. vulgaris* Hildenborough and *D. alaskensis* G20. Through these experiments we varied sulfate concentrations from 1-100% of modern values and modulated the electron delivery rate over an order of magnitude in order to induce varying degrees of limitation in electron availability. These experiments thus target the two primary controls on sulfate reduction – electron donation rate (lactate flux) and reception (sulfate availability) – and map onto distinct geological questions. For example, in the case of sulfate availability, the difference in isotopic composition between Proterozoic sulfates and sulfides is often inferred as related to $[SO_4^{2-}]$; our experiments directly address this assumption as they span the presumed $[SO_4^{2-}]$ for that time interval (0.5-5 mM). Our entire data set presents fractionation that in $^{34}S/^{32}S$ range from the ordinary (< 25‰) to the extraordinary (> 50‰), and can be contoured by electron consumption rates. When paired with the minor isotope data, the flux of sulfur through a bacterium can be more specifically solved for. This is in part because of the steady-state character of the experiments and through additional insight gained from oxygen isotope geochemistry. In the case of the oxygen isotope work, we lean on new experimental calibrations of the sulfite-water isotope equilibrium conducted over a range of temperatures and pH (data presented herein). Together with an updated metabolic model (*2*), this study allows for the internal operation of the metabolism to be solved.

Through the tight constraints allowed by our experimental design, and with the direct measurement of all sulfur bearing phases present in the reactor at each time point (satisfying elemental and isotopic mass-balance), we link electron utilization to isotopic fractionation (*3*) in a manner that allows for geological records to be more fully interpreted. This work also helps to open the 'black box' of large fractionations produced by sulfate reduction through solid physiological and geochemical constraints. The sum of the information gained through this work will allow Proterozoic and Phanerozoic oxidant budgets to become more accessible.

(*1*) D. E. Canfield, in *Stable Isotope Geochemistry*. (2001) 607-636. (*2*) A. S. Bradley et al., *Geobiology* **9**, 446 (2011). (*3*) L. A. Chambers et al., *Canadian Journal of Microbiology* **21**, 1602 (1975).

Neutron scattering reveals conformations of the transcriptional regulator MerR in complex with its operator DNA

ALEXANDER JOHS[1*], STEPHEN J. TOMANICEK[1], HAO-BO GUO[1], ANNE O. SUMMERS[2], AND LIYUAN LIANG[1]

[1]Oak Ridge National Laboratory, Oak Ridge, TN, U.S.A., johsa@ornl.gov (* presenting author)

[2]University of Georgia, Athens, GA, U.S.A.

Bacterial resistance to heavy metals is controlled by metal-responsive transcriptional regulators. For example, bacterial resistance to inorganic and organic mercury compounds is conferred by the *mer* operon, which is typically located on transposons or plasmids [1,2]. These proteins are involved in Hg(II) import, proteolysis of organomercurials and Hg(II) reduction to Hg(0). Expression of the *mer* operon genes is controlled by the transcriptional repressor-activator MerR.

How Hg(II) binding affects the changes in the conformation of MerR, which in turn propagate through DNA contacts to its operator DNA (MerOP) is unknown. In this study we investigate Hg(II)–induced conformational changes of MerOP in complex with its regulator MerR to reveal the transcription control mechanism conferred by MerR. Experimentally, we purified MerR and prepared a complex with a 23bp MerOP dsDNA construct. In vivo, MerR tightly binds to MerOP in a region of dyad symmetry between the -10 and -35 RNA polymerase recognition sites. In the absence of Hg(II), RNA polymerase binds to its promoter and forms a stable pre-initiation complex with dimeric MerR acting as a repressor preventing RNA polymerase from accessing the -10 recognition site. In the experiments, we examined the MerR-MerOP complex in the presence and absence of Hg(II) using small-angle neutron scattering (SANS) (Fig. 1). A contrast variation series allowed us to detect changes in the conformation of MerR and MerOP, respectively. Homology modeling and molecular dynamics simulations were used to generate atomic resolution models to interpret the data. The results provide insights on the allosteric change in MerR triggered by Hg(II), which causes a reorientation of the -10 recognition site and ultimately initiation of transcription by RNA polymerase [3].

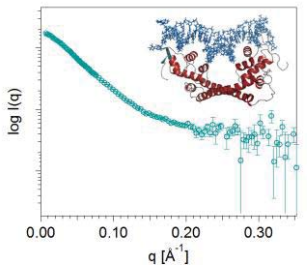

Figure 1: Small angle neutron scattering intensities I(q) vs momentum transfer (q) in 100% D_2O buffer and a model of the MerR-MerOP complex.

[1] Barkay et al. (2003) *FEMS Microbiol Rev* **27**, 385-384.
[2] Summers et al. (1986) *Annu Rev Microbiol* **40**, 607-634.
[3] Ansari et al. (1995) *Nature* **374**, 371-375.